AMERICAN SOCIETY FOR MICROBIOLOGY | Applied and Environmental Microbiology®

GENETICS AND MOLECULAR BIOLOGY

Phenylacetyl Coenzyme A, Not Phenylacetic Acid, Attenuates CepIR-Regulated Virulence in *Burkholderia cenocepacia*

Tasia Joy Lightly,[a] Kara L. Frejuk,[a] Marie-Christine Groleau,[c] Laurent R. Chiarelli,[d] Cor Ras,[e] Silvia Buroni,[d] Eric Déziel,[c] John L. Sorensen,[f] Silvia T. Cardona[a,b]

[a]Department of Microbiology, University of Manitoba, Winnipeg, Canada
[b]Department of Medical Microbiology and Infectious Diseases, University of Manitoba, Winnipeg, Canada
[c]Armand-Frappier Santé Biotechnologie Center, Institut National de la Recherche Scientifique, Laval, Canada
[d]Department of Biology and Biotechnology Lazzaro Spallanzani, University of Pavia, Pavia, Italy
[e]Department of Biotechnology, Delft University of Technology, Delft, The Netherlands
[f]Department of Chemistry, University of Manitoba, Winnipeg, Canada

ABSTRACT During phenylalanine catabolism, phenylacetic acid (PAA) is converted to phenylacetyl coenzyme A (PAA-CoA) by a ligase, PaaK, and then PAA-CoA is epoxidized by a multicomponent monooxygenase, PaaABCDE, before further degradation through the tricarboxylic acid (TCA) cycle. In the opportunistic pathogen *Burkholderia cenocepacia*, loss of *paaABCDE* attenuates virulence factor expression, which is under the control of the LuxIR-like quorum sensing (QS) system, CepIR. To further investigate the link between CepIR-regulated virulence and PAA catabolism, we created knockout mutants of the first step of the pathway (PAA-CoA synthesis by PaaK) and characterized them in comparison to a *paaABCDE* mutant using liquid chromatography-tandem mass spectrometry (LC-MS/MS) and virulence assays. We found that while loss of PaaABCDE decreased virulence, deletion of the *paaK* genes resulted in a more virulent phenotype than that of the wild-type strain. Deletion of either *paaK* or *paaABCDE* led to higher levels of released PAA but no differences in levels of internal accumulation compared to the wild-type level. While we found no evidence of direct *cepIR* downregulation by PAA-CoA or PAA, a low-virulence *cepR* mutant reverted to a virulent phenotype upon removal of the *paaK* genes. On the other hand, removal of *paaABCDE* in the *cepR* mutant did not impact its attenuated phenotype. Together, our results suggest an indirect role for PAA-CoA in suppressing *B. cenocepacia* CepIR-activated virulence.

IMPORTANCE The opportunistic pathogen *Burkholderia cenocepacia* uses a chemical signal process called quorum sensing (QS) to produce virulence factors. In *B. cenocepacia*, QS relies on the presence of the transcriptional regulator CepR which, upon binding QS signal molecules, activates virulence. In this work, we found that even in the absence of CepR, *B. cenocepacia* can elicit a pathogenic response if phenylacetyl-CoA, an intermediate of the phenylacetic acid degradation pathway, is not produced. Instead, accumulation of phenylacetyl-CoA appears to attenuate pathogenicity. Therefore, we have discovered that it is possible to trigger virulence in the absence of CepR, challenging the classical view of activation of virulence by this QS mechanism. Our work provides new insight into the relationship between metabolism and virulence in opportunistic bacteria. We propose that in the event that QS signaling molecules cannot accumulate to trigger a pathogenic response, a metabolic signal can still activate virulence in *B. cenocepacia*.

KEYWORDS *Burkholderia*, *Burkholderia cenocepacia*, *Burkholderia cepacia* complex, CepIR, CepR, phenylacetyl-CoA, metabolic regulation, phenylacetate, phenylacetic acid, quorum sensing

Citation Lightly TJ, Frejuk KL, Groleau M-C, Chiarelli LR, Ras C, Buroni S, Déziel E, Sorensen JL, Cardona ST. 2019. Phenylacetyl coenzyme A, not phenylacetic acid, attenuates CepIR-regulated virulence in *Burkholderia cenocepacia*. Appl Environ Microbiol 85:e01594-19. https://doi.org/10.1128/AEM.01594-19.

Editor Edward G. Dudley, The Pennsylvania State University

Address correspondence to Silvia T. Cardona, Silvia.Cardona@umanitoba.ca.

Received 22 July 2019
Accepted 30 September 2019
Accepted manuscript posted online 4 October 2019
Published 27 November 2019

Intercellular communication in bacteria, or quorum sensing (QS), relies on the production and detection of signaling molecules to regulate gene expression in a cell density-dependent manner (1, 2). In many Gram-negative bacteria, LuxI homologs synthesize *N*-acyl homoserine lactones (AHLs) as signaling molecules. These small diffusible molecules accumulate extracellularly as the population increases until the concentration is sufficient for AHLs to return into the cell where they bind LuxR-type transcriptional regulators. Complexing of the AHL to the LuxR homolog results in a conformational change that alters the ability of the transcriptional regulator to bind DNA and regulate gene expression (3). Many of the genes regulated by QS control expression of virulence traits, which are important for bacteria to establish infection (4).

A bacterium with a LuxIR-type QS system is *Burkholderia cenocepacia*, a member of the *Burkholderia cepacia* complex (5). The strain *B. cenocepacia* K56-2, isolated from the sputum of a cystic fibrosis patient, has two complete LuxIR-type QS systems, CepIR and CciIR, and one orphan transcriptional regulator, CepR2 (5, 6). The regulons of CepR and CciR have been examined, and a large number of the genes that are regulated are linked to virulence (7). While CepR and CciR have separate regulons, certain genes are regulated by both in a reciprocal manner (7). CepR positively regulates gene expression, whereas CciR is responsible for negative gene regulation (7). While these two systems regulate certain genes in a reciprocal manner, rather than hierarchically in the manner of those of *Pseudomonas aeruginosa*, the transcription of both *cepI* and *cciIR* is dependent on CepR, and in turn CciR negatively regulates the expression of *cepI* (7, 8). CepR and CciR both positively regulate their canonical autoinducer synthase and negatively regulate their own transcription (8, 9). CepI mainly produces *N*-octanoyl homoserine lactone (C_8-HSL) with slight production of *N*-hexanoyl homoserine lactone (C_6-HSL), whereas CciI synthesizes C_6-HSL with slight secondary production of C_8-HSL (8, 10). CepR2 lacks a cognate AHL synthase and has been shown to regulate known QS-regulated genes independent of a signaling molecule (11).

Several lines of evidence point to metabolic adaptation as an important component of virulence regulation (12–15). In this context, high levels of phenylacetic acid (PAA) have been linked to evasion of the immune response by *Acinetobacter* (16), inhibition of pathogenicity of the fungus *Rhizoctonia solani* (17), and downregulation of virulence gene expression in *B. cenocepacia* (18). The PAA degradation pathway is a central route by which diverse aromatic compounds, such as phenylalanine, converge and are directed to the tricarboxylic acid (TCA) cycle (19). In *Escherichia coli* K-12, PAA is converted to phenylacetyl coenzyme A (PAA-CoA) by the action of a phenylacetyl-CoA ligase, PaaK (19). The conversion to PAA-CoA by PaaK can be reverted to PAA by the action of PaaI, a thioesterase, to prevent accumulation should downstream steps be disrupted (20). Next, PAA-CoA is epoxidized by the multicomponent monooxygenase PaaABCDE and then further degraded into succinyl-CoA and acetyl-CoA (19).

We previously found that CepIR-regulated virulence traits and *cepI* and *cepR* promoter activity were downregulated in a *B. cenocepacia* mutant of the *paaABCDE* operon that released PAA (18). We also demonstrated that PAA could be produced to detectable levels in wild-type *B. cenocepacia* K56-2 under certain conditions, suggesting a potential physiological role of the regulation of virulence by this molecule (21). However, the PaaABCDE mutant is still able to degrade PAA to PAA-CoA. Therefore, the metabolite responsible and the mechanism of the regulation of virulence by accumulated PAA-metabolites are not known. In this work, we further characterized mutants of the PAA degradation pathway to show that the loss of PaaK function increases virulence, suggesting that PAA-CoA is responsible for the attenuation phenotype. While we found no evidence of a direct effect of PAA-CoA on CepI activity or the formation of CepR:C_8-HSL complexes, our results are consistent with a parallel mechanism that uses PAA-CoA, or a derivative, as a regulatory ligand and competes with the CepIR complex to regulate virulence.

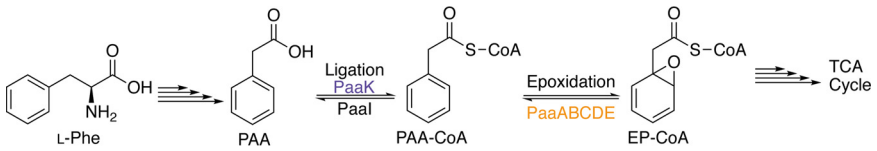

FIG 1 The proposed phenylacetic acid (PAA) degradation pathway in *B. cenocepacia*. Based on the pathway described in *E. coli* and *Pseudomonas* by Teufel et al. (19), phenylalanine (Phe) is degraded to PAA, and the first step of the pathway is the conversion of PAA to phenylacetyl-CoA (PAA-CoA) by the phenylacetyl-CoA ligase PaaK. The phenylacetyl-CoA thioesterase, PaaI, can reversibly convert PAA-CoA back to PAA to prevent toxic accumulation of the epoxide if the downstream pathway is blocked. PAA-CoA is epoxidized by the ring 1,2 phenylacetyl-CoA epoxidase, PaaABCDE, forming ring-1,2-epoxyphenylacetyl-CoA or epoxide (EP-CoA). The epoxide is further degraded to components of the TCA cycle, acetyl-CoA and succinyl-CoA.

RESULTS

Creation and phenotypic characterization of a *paaK* double mutant. Previously, we demonstrated a link between the attenuation of *B. cenocepacia* K56-2 Δ*paaABCDE* and the release of PAA (18). However, the interruption of the pathway at this step could also result in an accumulation of PAA-CoA because PAA is converted to PAA-CoA by a PaaK ligase (Fig. 1). To determine the role of each of these molecules in the attenuation of virulence, we characterized a *paaK* mutant that should produce only PAA and compared it to the *paaABCDE* mutant. Similar to the reference strain *B. cenocepacia* J2315 (22), K56-2 harbors two similar but not identical phenylacetyl-CoA ligases, PaaK1 and PaaK2 (23). We created markerless deletion mutants of *paaK1* (BCAL0404) and *paaK2* (BCAM1711). Knockout mutants of the other *paaK* gene were then made in each background, resulting in two independently made double knockouts, which we have named the Δ*paaK1* Δ*paaK2* and Δ*paaK2* Δ*paaK1* strains.

To confirm the interruption of the PAA pathway, K56-2 and mutants were grown on lysogeny broth (LB) medium and M9 minimal medium with glucose or PAA as a sole carbon source. No growth defect was observed in LB or glucose medium (Fig. 2A and B). Both *paaK* single knockout mutants were also able to grow on PAA as a sole carbon source to wild-type levels, indicating that PAA can be used as a substrate for both ligases (Fig. 2B). While mutants were able to grow normally on glucose as a sole carbon source, the *paaK* double knockout mutants (Δ*paaK1* Δ*paaK2* and Δ*paaK2* Δ*paaK1* strains) were unable to grow on PAA (Fig. 2B). Growth was complemented with a plasmid containing a rhamnose-inducible *paaK2* (BCAM1711) (see Fig. S2 in the supplemental material), confirming that the interruption of the pathway in these mutants was caused by the deletion of *paaK*. Therefore, mutants with full interruption of the pathway (Δ*paaABCDE*, Δ*paaK1* Δ*paaK2*, and Δ*paaK2* Δ*paaK1* strains) were unable to grow on PAA as a sole carbon source. Single deletion mutants of the *paaK* ligases (Δ*paaK1* and Δ*paaK2* strains) grew to wild-type levels on PAA, indicating that the pathway is not interrupted in these strains.

The PaaABCDE mutant has been shown to accumulate extracellular PAA due to the interruption of the pathway (18), but the concentrations of intracellular PAA and PAA-CoA were unknown. Intracellular and extracellular concentrations of both PAA and PAA-CoA were measured with ion-pair reversed-phase ultrahigh-performance liquid chromatography tandem mass spectrometry (IP-RP-UHPLC-MS/MS) using the differential method (24–26). In general, high levels of PAA were found extracellularly rather than intracellularly. The average extracellular concentrations of PAA in the wild-type, Δ*paaABCDE*, Δ*paaK1* Δ*paaK2*, and Δ*paaK2* Δ*paaK1* supernatants were 37.3, 357.0, 107.3, and 93.9 μM, respectively (Fig. 2C), whereas the average values for intracellular PAA in the same strains were 6.0, 2.0, 1.7, and 8.0 μM (Fig. 2D). When we examined the concentrations of PAA-CoA, we found that the average extracellular levels of PAA-CoA were below or near the limit of detection for all strains, as expected for a CoA molecule that cannot transverse cell membranes. However, PAA-CoA accumulated intracellularly to levels slightly above the limit of detection (Fig. 2E). The intracellular levels of PAA-CoA (Fig. 2F) were higher in the Δ*paaABCDE* mutant (0.94 μM) than in the PaaK

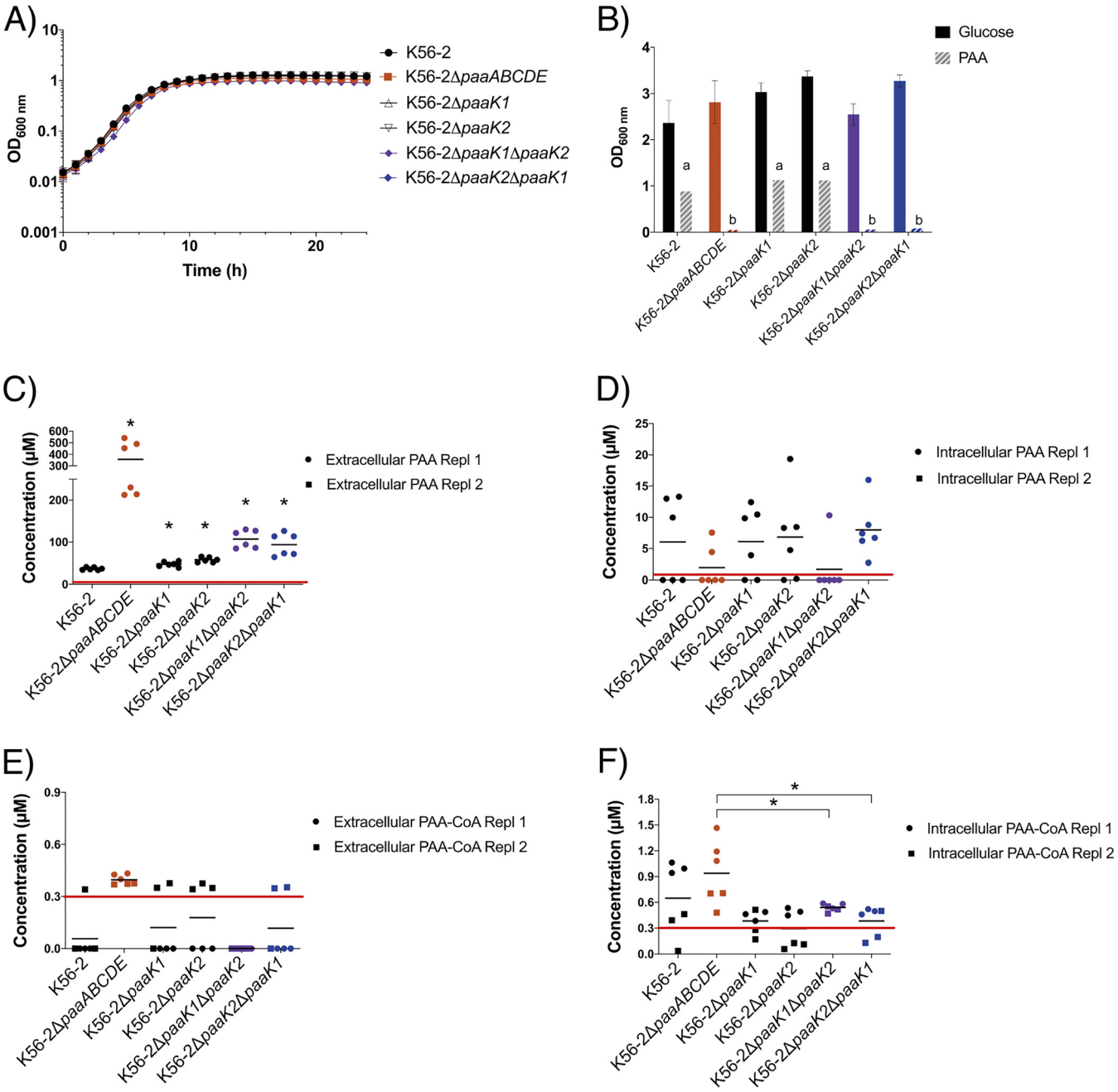

FIG 2 Characterization of the growth and metabolite production of *B. cenocepacia* PAA pathway mutants. (A) Growth curves of *B. cenocepacia* K56-2 PAA pathway mutants on LB medium. (B) Endpoint growth of *B. cenocepacia* K56-2 PAA pathway mutants. Strains were cultured on M9 medium with 25 mM glucose or with 5 mM PAA as the sole carbon sources for 48 h, and the OD_{600} was measured. Error bars represent standard deviations for three biological replicates (a, no significant difference; b, $P \leq 0.05$ as determined by Student's *t* test (two-tailed) compared to growth on PAA of K56-2. (C to F) Cultures were grown to late exponential phase, and equal volumes of whole-cell cultures and filtered supernatants were frozen, extracted with 75% (vol/vol) ethanol, and analyzed with ion-pair reversed-phase ultrahigh-performance liquid chromatography tandem mass spectrometry (IP-RP-UHPLC-MS/MS). Extracellular and intracellular levels of PAA and PAA-CoA are shown. A horizontal line represents the mean and an asterisk denotes a *P* value of ≤ 0.05, as determined by Student's *t* test (two-tailed) compared to results with K56-2 (C) or the Δ*paaABCDE* mutant (F). The limits of detection for PAA (1 μM) and PAA-CoA (0.3 μM) are indicated by red lines. Two biological replicates (Rep) with three technical replicates each were performed.

mutants (0.54 μM and 0.38 μM). However, the low-micromolar amounts detected and the high variability between biological replicates made it challenging to establish clear differences between the PAA-CoA content of the wild type and the PAA degradation mutants.

To determine how interruption of each of the two consecutive steps of PAA degradation could affect QS-regulated virulence traits, the killing ability of PAA path-

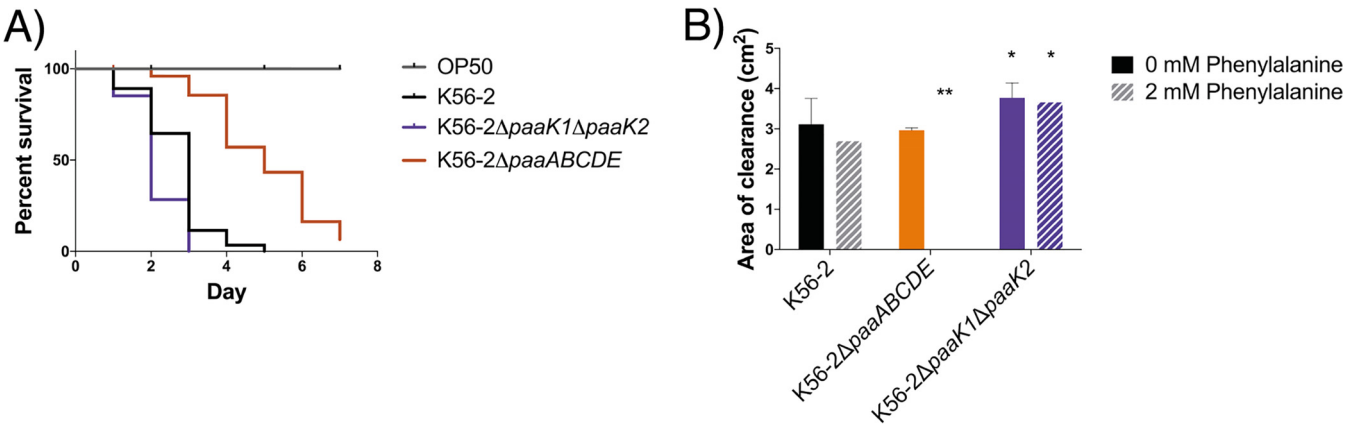

FIG 3 The Δ*paaK1* Δ*paaK2* mutant is more virulent than the wild type in *C. elegans* and has higher proteolytic activity. (A) Slow-killing assays with *C. elegans* over a period of 7 days show that the Δ*paaK1* Δ*paaK2* mutant kills *C. elegans* in a similar time frame as the wild type, whereas the nematodes exposed to the Δ*paaABCDE* mutant have increased survival ($n = \sim 70$ to 100 nematodes per strain). The increased killing ability of the Δ*paaK1* Δ*paaK2* mutant compared to that of the wild type was determined as significant according to a log rank test ($P < 0.001$). Three biological replicates were performed. (B) Proteolytic activity was measured as the area of the zone of clearance (excluding colonies) on agar containing 2% skim milk with or without the addition of 2 mM phenylalanine. The error bars represent the standard deviations of three independent experiments. *, $P < 0.05$; **, $P < 0.01$ (comparing results to those with the wild type).

way mutants was compared to that of the wild type in slow-killing assays, which quantify the survival of gut-infected nematodes fed on the respective mutants (Fig. 3A). As previously seen, the Δ*paaABCDE* mutant-exposed nematodes had a higher survival rate than those fed on K56-2 ($P < 0.001$). Surprisingly, the nematodes exposed to the Δ*paaK1* Δ*paaK2* mutant showed only 31% (±19%) survival on day 2. This was an increase in pathogenicity compared to that of K56-2, which had 66% (±10%) survival on day 2 ($P < 0.0001$). This virulent phenotype was also observed in nematodes fed with the Δ*paaK2* Δ*paaK1* mutant (Fig. S3A) but not in those fed with the single *paaK* deletion mutants (Fig. S3B).

To further investigate the opposite virulence phenotypes of the Δ*paaABCDE* and Δ*paaK1* Δ*paaK2* mutants, we measured the exoprotease activity of both strains, a well-studied virulence trait of *B. cenocepacia* that is regulated by CepIR (10, 27). To ensure that PAA-related metabolites could be produced, we added the precursor phenylalanine to the 2% skim milk agar used for the exoprotease assay, as previously performed (18). In the absence of phenylalanine, the proteolytic activity of the Δ*paaABCDE* mutant was similar to that of K56-2. However, when phenylalanine was added to the medium, the proteolytic activity of the Δ*paaABCDE* mutant was abolished (Fig. 3B). On the other hand, the proteolytic activities of the Δ*paaK1* Δ*paaK2* and Δ*paaK2* Δ*paaK1* strains were higher than the activity of K56-2, regardless of the addition of phenylalanine (Fig. 3B and Fig. S3C). This is in agreement with the results from the slow-killing assays where only the Δ*paaABCDE* mutant was attenuated for virulence while the Δ*paaK1* Δ*paaK*2 and Δ*paaK2* Δ*paaK1* mutants were more pathogenic than the wild type. Together, we observed no correlation between extracellular levels of PAA and pathogenicity (Fig. S4).

PAA-CoA has no effect on CepR and CepI function *in vitro*. Because PAA-CoA synthesis is interrupted in the *paaK* mutants but not in the *paaABCDE* mutant, we hypothesized that PAA-CoA was responsible for attenuating virulence. As the Δ*paaABCDE* mutant is attenuated for virulence traits that are under the control of the CepIR quorum sensing system (28), we focused our attention on a possible direct effect of PAA-CoA on CepIR. In addition, the Δ*paaABCDE* mutant had decreased *cepI* and *cepR* promoter activity and AHL signaling (18). Specifically, we asked whether PAA-CoA could (i) inhibit the formation of CepR:AHL complexes, (ii) inhibit the enzymatic activity of CepI, and/or (iii) indirectly affect an upstream regulator.

To address the first question, we built a reporter system similar to that commonly used to identify quorum sensing inhibitors (29). *E. coli* W14 was selected as our reporter

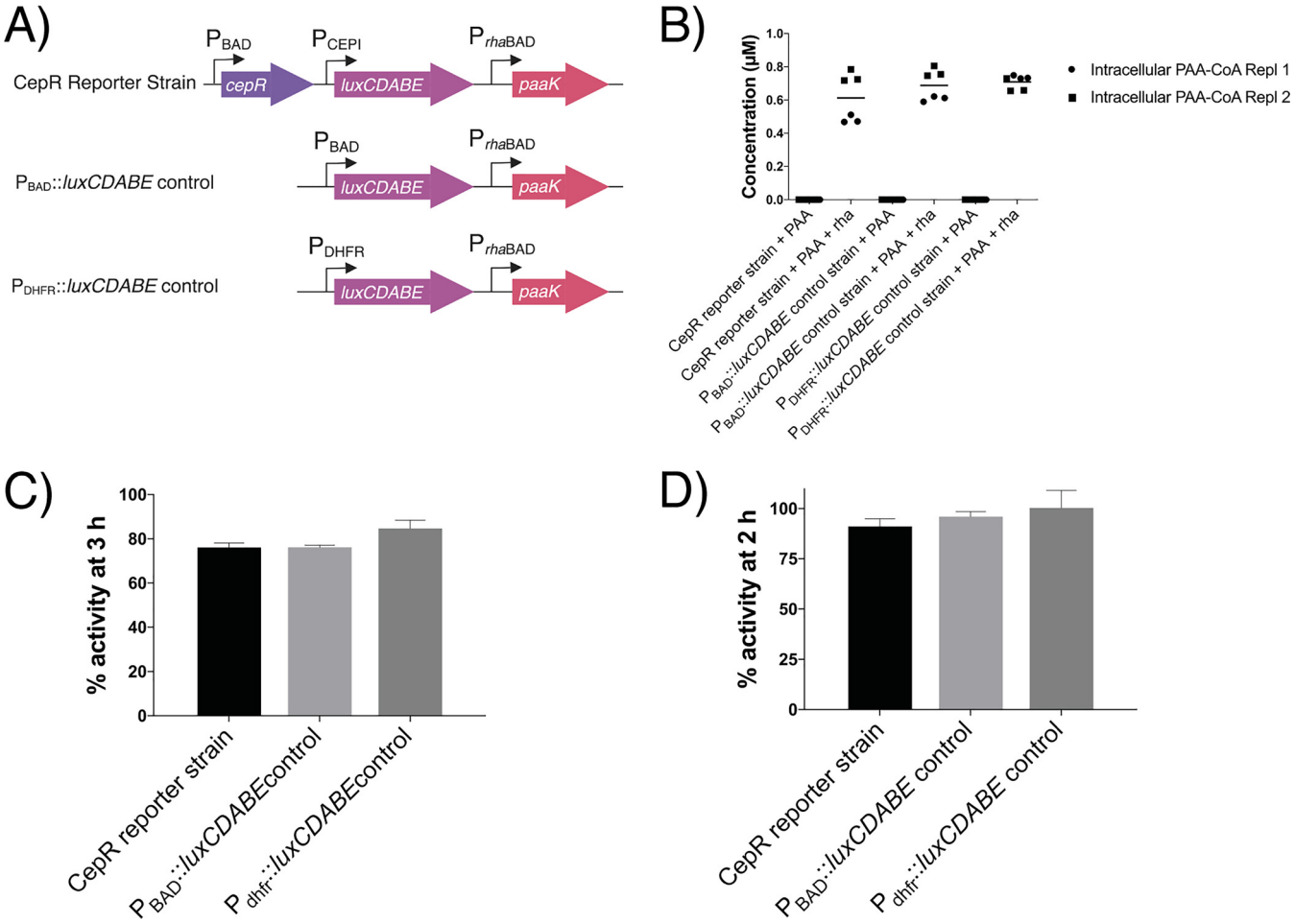

FIG 4 Neither PAA nor PAA-CoA affects the formation of CepR:C_8-HSL complexes. (A) The CepR reporter strain and control strains used. Regulatory genes *araC* (for P_{BAD}) and *rhaSR* (for $P_{rha\ BAD}$) were excluded from the figure for simplicity. (B) In the presence of 0.01% rhamnose (Rha), 0.5 mM PAA was converted to PAA-CoA by the PaaK ligase in the CepR reporter strain. For the reporter system, 0.2% arabinose was used to induce the expression of *cepR*, and the calculated EC_{50} of C_8-HSL (20 nm) was used to activate the system. (C) To test the effect of PAA-CoA, 0.5 mM PAA and 0.01% rhamnose were added, and the percent activity (activity in the presence of rhamnose compared to that in the absence of rhamnose) was determined at 3 h. PAA-CoA had no effect on the CepR reporter strain compared to that of the effect on control strains. (D) PAA itself was tested at various concentrations from 0.1 to 1 mM (0.1 mM shown here), and percent activity was calculated for the presence of PAA compared to activity in the absence of PAA at 2 h. No effect was observed compared to levels in the control strains. The error bars represent the standard deviations of three independent experiments.

strain as it lacks the PAA pathway genes (30, 31), ensuring that the exogenously added PAA-related compounds would not be degraded. Using arabinose-inducible expression of *cepR* (BCAM1868), we created a reporter strain that responds to CepR:AHL complexes by activating the *cepI* promoter, which controls the expression of luminescence genes *luxCDABE* (Fig. 4A). Expression of luminescence is decreased in the presence of an inhibitor of the formation of CepR:AHL complexes. However, PAA-CoA cannot be added exogenously to cultures because it is too large to cross the membrane. Therefore, we created a plasmid that contains the *E. coli* W *paaK* ligase gene (ECW_RS07845) under the control of a rhamnose-inducible promoter. In the presence of rhamnose, PaaK converts exogenously added PAA to PAA-CoA, as confirmed by IP-RP-UHPLC-MS/MS (Fig. 4B). To ensure that any effects we saw were not due to an inhibition of the arabinose-inducible promoter or luminescence itself, we created two control strains that contain either the arabinose-inducible P_{BAD} promoter or a constitutive promoter, *dhfr*, controlling the *luxCDABE* genes.

Using this reporter system (W14/pTL7/pTL5/pTL22 is referred to from here on as the CepR reporter strain) (Fig. 4A), we observed that although there was inhibition of luminescence in the presence of PAA-CoA, the level of inhibition was similar to the levels of the control strains (Fig. 4C). Similarly, PAA itself also had no effect on the

TABLE 1 CepI activity is not inhibited by the presence of PAA or PAA-CoA

Condition	Enzyme activity ± SD (U/mg)[a]
C_8-ACP + SAM	3.46 ± 0.12
C_8-ACP + SAM + 200 μM PAA	3.29 ± 0.21
C_8-ACP + SAM + 200 μM PAA-CoA	3.04 ± 0.29

[a]One unit (U) is defined as the amount of the enzyme that catalyzes the conversion of one micromole of DCPIP per minute at 37°C.

system (Fig. 4D). In summary, these results show that PAA-CoA and PAA do not directly affect CepI activity or CepR:C_8-HSL formation.

To analyze if PAA or PAA-CoA inhibits the enzymatic activity of CepI, we used recombinant CepI in the presence of dichlorophenolindophenol (DCPIP) to spectrophotometrically measure the activity of CepI (32). CepI catalyzes the formation of C_8-HSL from octanoyl-acyl carrier protein (C_8-ACP) and *S*-adenosyl methionine (SAM). During this reaction DCPIP is reduced, resulting in a color change that can be used to measure activity of CepI. Enzyme activity showed no change in the presence of 200 μM PAA-CoA or PAA (Table 1), suggesting that neither molecule directly inhibits the activity of CepI.

As our data did not show a direct effect of PAA-CoA on the CepIR QS system but *cepI* and *cepR* promoter activity was decreased in the PaaABCDE mutant (18), we hypothesized that PAA-CoA may indirectly affect an upstream regulator of the CepIR QS system. If this was the case, we predicted that the differences in pathogenicity between the Δ*paaABCDE* and the Δ*paaK1* Δ*paaK2* mutant strains would be explained by differential expression of *cepI* and *cepR*. Using stationary-phase cultures, we measured the transcript levels of *cepI* and *cepR* and the levels of C_8-HSL in the PAA pathway mutants and compared them to the levels in the wild type. Surprisingly, the Δ*paaABCDE* and the Δ*paaK1* Δ*paaK2* mutants had wild-type levels of *cepI* and *cepR* transcription (Fig. 5A and Fig. S5A) despite the striking differences in their virulence phenotypes and contradicting our previous results where reporter systems measured decreased *cepI* and *cepR* promoter activity and decreased AHL signaling (18). This suggested that the attenuation of the Δ*paaABCDE* mutant is independent of the transcription of the CepIR QS system. To confirm the wild-type transcription levels of our mutants, we measured the levels of AHL molecules in each strain. Similar to the transcription levels, the levels of C_8-HSL, taken from stationary-phase samples, did not correlate with the decreased virulence of our PAA pathway mutants (Fig. 5B and Fig. S5B). However, both the Δ*cepI*

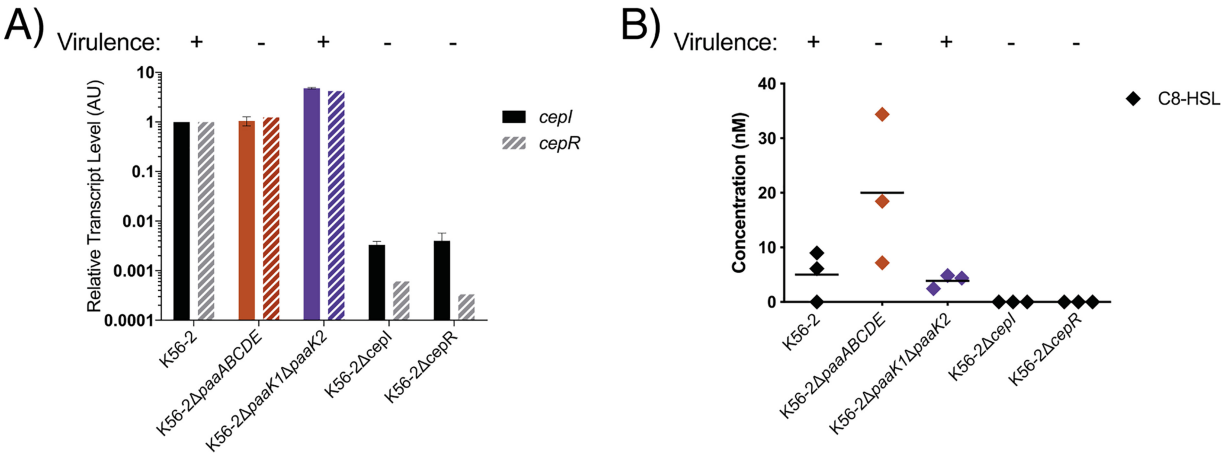

FIG 5 Transcription of *cepI* and *cepR* and C_8-HSL production are not decreased in any of the PAA pathway mutants. (A) RT-qPCR shows that *cepI* and *cepR* gene expression is not decreased in the PAA pathway mutants compared to that in the wild type. (B) C_8-HSL levels were not decreased in any of the mutants, but C_8-HSL levels were higher in the Δ*paaABCDE* mutant. Virulence of strains in both *C. elegans* assays and exoprotease activity assays is denoted above the graphs per the results from the experiment shown in Fig. 3. AU, arbitrary units.

and Δ*cepR* mutants had no measurable C_8-HSL, which is consistent with their lack of virulence (Fig. 5B).

The CepR-independent virulence of PaaK knockout mutants is mediated by the presence/absence of PAA-CoA. Transcription of *cepI* and *cepR* is not decreased in PAA pathway mutants, and C_8-HSL is present in the mutants, yet the virulence factors attenuated in the Δ*paaABCDE* mutant (pathogenicity in *Caenorhabditis elegans* and exoprotease activity) are known to be under the control of the CepIR system. To further understand how the PAA pathway may regulate QS-related virulence without affecting *cepIR* transcription, we created markerless deletions of *cepI* and *cepR* in the PAA pathway deletion mutant backgrounds. We reasoned that if PAA-related regulation of virulence was completely independent of CepI and CepR activity, then deletion of *cepI* and *cepR* in a Δ*paaABCDE* strain background should show an additive attenuation effect. Similarly, deletion of *cepI* and *cepR* in a Δ*paaK1* Δ*paaK2* mutant background should show the same degree of attenuation as the *cepI* and *cepR* deletions in a wild-type background. Once we had created knockout mutants of *cepI* and *cepR* for each PAA pathway mutant in parallel with *cepI* and *cepR* deletions in wild-type K56-2, we analyzed their growth and found no defect when strains were grown in LB medium over 24 h (Fig. S6). Next, we used virulence assays to determine if the CepIR QS system was needed for the regulation of their QS. The virulence levels of the *cepI* and *cepR* knockout mutants in wild-type and PAA mutant backgrounds were compared in slow-killing assays (Fig. 6A and B and Fig. S7A and B). Both *cep* QS mutants in the Δ*paaABCDE* background were more attenuated for virulence than the Δ*paaABCDE* strain (Fig. S7A). However, they failed to show an additive effect (Fig. S7A). Moreover, while the Δ*paaK1* Δ*paaK2* Δ*cepI* mutant was as attenuated as Δ*cepI*, the Δ*paaK1* Δ*paaK2* Δ*cepR* mutant was not, showing that the pathogenic phenotype was independent of CepR (Fig. 6A and B). This was mirrored in the Δ*paaK2* Δ*paaK1* Δ*cepR* mutant (Fig. S7B). This is surprising considering that the *cepR* deletion in the wild type and the *paaABCDE* mutant has a severe attenuation (Fig. S7A).

Corroborating the results of the *C. elegans* assay, the Δ*paaK1* Δ*paaK2* Δ*cepR* mutant had wild-type levels of proteolytic activity whereas the Δ*paaK1* Δ*paaK2* Δ*cepI* mutant had none (Fig. 6C and Fig. S7C). The only difference between the Δ*paaK1* Δ*paaK2* Δ*cepR* mutant and the *cepR* mutant is the presence of PAA. If PAA were responsible for the elimination of the *cepR* attenuation, the Δ*paaABCDE* Δ*cepR* mutant should be pathogenic, but our results show that it is not.

To further understand the virulence of the Δ*paaK1* Δ*paaK2* Δ*cepR* mutant, we examined the expression levels of *cepI* and *cepR* and the levels of C_8-HSL in the mutants. While transcription of *cepR* is abolished in Δ*cepI*, it is restored to wild-type levels when the deletion of *cepI* occurs in a Δ*paaK1* Δ*paaK2* or Δ*paaABCDE* mutant background (Fig. 6D; see also Fig. S7D for Δ*paaK2* Δ*paaK1*). Therefore, PAA, which is present in both PAA pathway mutants, restores *cepR* transcription but not pathogenicity because there is no CepI and no C_8-HSL (Fig. 6F). When *cepI* transcript levels were analyzed in Δ*cepR* in the wild type and PAA degradation mutant backgrounds, the transcription of *cepI* was downregulated in the CepR mutant, as expected. Similarly, *cepI* transcription was reduced in the attenuated Δ*paaABCDE* Δ*cepR* mutant and in the pathogenic Δ*paaK1* Δ*paaK2* Δ*cepR* mutant (Fig. 6E; see also Fig. S7E for the Δ*paaK2* Δ*paaK1* Δ*cepR* mutant). The lack of C_8-HSL in both the Δ*paaK1* Δ*paaK2* Δ*cepI* and Δ*paaK1* Δ*paaK2* Δ*cepR* mutants (Fig. 6F) suggests that the pathogenicity of the Δ*paaK1* Δ*paaK2* Δ*cepR* mutant is independent of *cepI*. This was mirrored in the Δ*paaK2* Δ*paaK1* Δ*cepR* mutant (Fig. S7F).

Deletions of the *cepI* and *cepR* genes in the PAA pathway mutant backgrounds allowed us to determine that the PAA pathway has an effect on CepIR-regulated virulence that is evident when CepI or CepR is absent. In this context, our results suggest that there is an alternative signaling pathway to activate virulence in the Δ*paaK1* Δ*paaK2* Δ*cepR* mutant. The opposite effects of the PaaK and PaaABCDE mutations with regard to pathogenicity and the striking differences that *paaK* and *paaABCDE* gene deletions have in the *cepR* mutant background suggest that

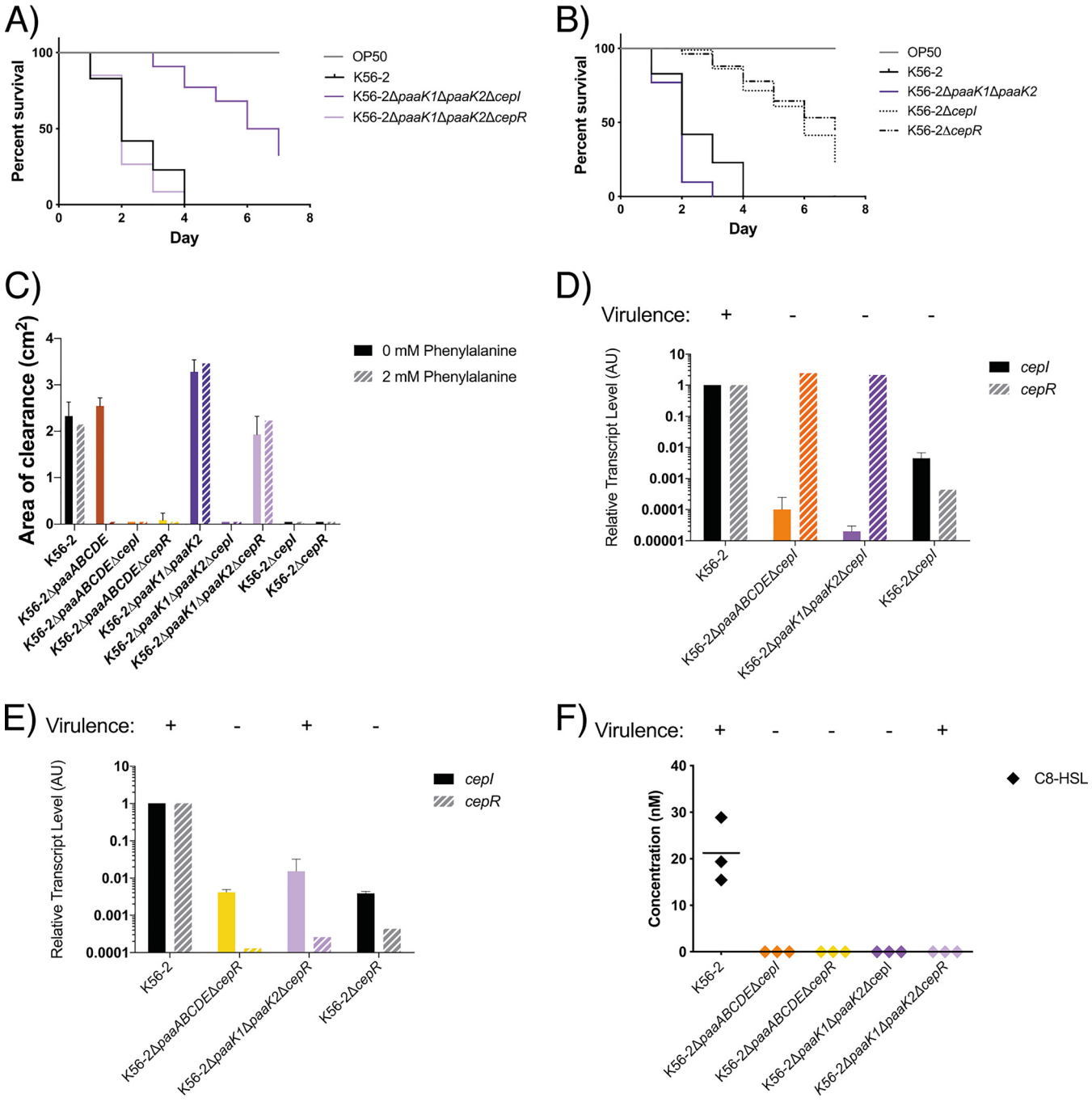

FIG 6 The virulence of the Δ*paaK1* Δ*paaK2* Δ*cepR* mutant is independent of the CepIR QS system. (A) The *cepI* and *cepR* mutations in a Δ*paaK1* Δ*paaK2* mutant have opposing levels of virulence. The Δ*paaK1* Δ*paaK2* Δ*cepR* mutant is as virulent as the wild type whereas the Δ*paaK1* Δ*paaK2* Δ*cepI* mutant is attenuated for virulence in *C. elegans*. (B) *cepI* and *cepR* mutants have similar levels of attenuation in *C. elegans*. Data shown in panels A and B are representative of three biological replicates ($n = \sim 70$ to 110 nematodes per strain). (C) The Δ*paaK1* Δ*paaK2* Δ*cepR* mutant has wild-type levels of proteolytic activity with or without phenylalanine whereas the Δ*cepR* mutant has decreased proteolytic activity. Proteolytic activity was measured as the area of the zone of clearance (excluding colonies) on agar containing 2% skim milk with or without the addition of 2 mM phenylalanine. (D) *cepR* transcription is restored to wild-type levels in the Δ*paaABCDE* Δ*cepI* and Δ*paaK1* Δ*paaK2* Δ*cepI* mutants, indicating that PAA restores *cepR* transcription. (E) *cepI* is downregulated in all of the Δ*cepR* mutants. (F) C_8-HSL levels were measured, and none of the QS mutants had detectable levels of C_8-HSL. The error bars represent the standard deviations of three independent experiments.

PAA-CoA, or a derivative, is the central molecule implicated in this alternative signaling pathway.

DISCUSSION

In *B. cenocepacia*, the attenuation of CepIR QS-regulated virulence traits in PAA pathway mutants was thought to be due to the accumulation of PAA (18). In line with

this finding, PAA has also been shown to regulate the virulence of other Gram-negative bacteria, *Acinetobacter baumannii* (16) and *Pseudomonas aeruginosa* (33, 34), two Gram-negative bacteria that also use LuxIR-type QS systems to regulate their virulence (35, 36). Previously, we demonstrated that the release of PAA in a *B. cenocepacia* mutant of the PAA pathway resulted in the inhibition of CepIR-regulated QS, a LuxIR-type system (18). However, the Δ*paaABCDE* mutant has the genes necessary to convert PAA to PAA-CoA (Fig. 1). Therefore, PAA or PAA-CoA could be the molecule responsible for the inhibition of CepIR-regulated QS.

To determine the molecule responsible, we attempted to create a mutant unable to accumulate PAA-CoA. The PaaK knockout mutant accumulated less PAA-CoA than the Δ*paaABCDE* mutant and was more virulent than the wild type, suggesting that the attenuated virulence could be due to the accumulation of PAA-CoA or a derivative. Another difference between these two mutants is that the PaaK knockout mutant released less PAA than the PaaABCDE mutant. Since PAA-CoA is the true inducer of the PAA pathway, the increased accumulation of PAA in the PaaABCDE mutant is likely due to induction of the upstream degradation pathway when PAA-CoA relieves the regulator, PaaR (37). Although our results show that the PaaABCDE mutant produces more PAA than both the Δ*paaK1* Δ*paaK2* and Δ*paaK2* Δ*paaK1* mutants, the accumulation of PAA is extracellular. There were no significant differences in the intracellular concentrations of PAA mutants compared with the level in the wild type, and the amounts were detected at levels very close to, or lower than, the smallest standard used for the calibration curve (8 μM). Therefore, any effect of PAA on virulence should be attributed to extracellular levels of PAA. However, this does not seem to be the case as exogenous addition of PAA to the *B. cenocepacia* wild type did not change its pathogenic phenotype (18).

We hypothesized that CepIR-regulated QS inhibition was achieved by one of three mechanisms: (i) direct inhibition of the enzymatic activity of CepI or its products, (ii) inhibition of the formation of CepR:C_8-HSL complex, or (iii) an indirect effect on an upstream regulator. Using an *E. coli* reporter system that cannot metabolize PAA, we examined the ability of PAA-CoA to act as a direct inhibitor of the CepIR QS system. We were able to observe strong but unspecific inhibition of luminescence by PAA and PAA-CoA, highlighting the importance of control strains when reporter systems are used to identify QS inhibitors. QS-regulated phenotypes often depend on other factors, and reporter strains using bioluminescence can be affected by the overall metabolic activity of the cell (29). In our system, the control strains had either the arabinose-inducible P_{BAD} promoter or the *dhfr* constitutive promoter controlling the expression of *luxCDABE* luminescence genes. First, in the presence of higher concentrations of PAA (above 1 mM), the expression of luminescence by the constitutive promoter was inhibited, suggesting a general effect on luminescence. Second, the concentration of rhamnose used to express *paaK*, 0.01% (wt/vol), inhibited the arabinose-inducible promoter. With these control strains, we were able to minimize the general effects on the reporter system and determine that neither PAA nor PAA-CoA has a direct effect on the formation of CepR:C_8-HSL complexes or on CepI activity.

Interestingly, we found that the attenuation of virulence in the Δ*paaABCDE* mutant did not correspond to decreased *cepI* and *cepR* transcription or C_8-HSL production. The lack of downregulation of either *cepI* or *cepR* in the Δ*paaABCDE* mutant was quite surprising because this contradicted the results from our plasmid-based reporter systems that showed decreased *cepI* and *cepR* promoter activity and decreased AHL signaling (18). To investigate this discrepancy, we introduced the plasmids with P_{cepI}::*luxCDABE* or P_{cepR}::*luxCDABE* to the Δ*paaK1* Δ*paaK2* and Δ*paaK2* Δ*paaK1* mutants and found decreased *cepI* and *cepR* promoter activity almost identical to that of the Δ*paaABCDE* mutant with the same plasmid-based reporter system (data not shown). This suggests that the PAA present in both of these mutants might have had a general effect on the reporter system itself. It is possible that PAA may affect the copy number of the plasmid or affect the metabolism of the cells in such a way that affects plasmid-based reporter strains, as previously shown in *E. coli* (38).

We initially focused our attention on *B. cenocepacia* CepIR because this QS system solely controls pathogenicity in *C. elegans* where the virulence attenuation of PAA degradation mutants was first characterized (22). However, current evidence suggests that a two-component system, RqpSR, is at the top of the hierarchy controlling both AHL- and *Burkholderia* diffusible signal factor (BDSF)-dependent QS systems (39, 40). The BDSF-dependent system uses *cis*-2-dodecenoic acid signaling molecule (BDSF) that regulates overlapping genes with the AHL QS system (41). We considered that the virulence of the Δ*paaABCDE* mutant may be attenuated through an indirect effect. However, RqpSR and BDSF both regulate the expression of *cepI*, which is not differentially regulated in the Δ*paaABCDE* mutant, nor was there decreased production of AHLs (39, 42). To determine if the attenuated virulence of the Δ*paaABCDE* strain could be independent of CepI and CepR activity, we created *cepI* and *cepR* mutants in the PAA pathway mutant backgrounds. If PAA-related regulation of virulence was independent of CepI and CepR activity, then we would see an additive effect on attenuation whereas in a *paaK* knockout mutant background, we expected to see a virulence phenotype similar to that of the same deletion in a wild-type strain. In the Δ*paaABCDE* QS mutants we saw no evidence of an additive effect as the QS mutations were dominant, leading to the same attenuated pathogenicity as the Δ*cepI* or Δ*cepR* mutant. Because the *cepI* and *cepR* mutations in the Δ*paaABCDE* strain did not have an additive effect, this suggests that the mechanism of attenuation involves the CepIR QS system without affecting the expression of the *cepI* and *cepR* genes. Recently, an analogue of BDSF was shown to inhibit the production of AHL signals in *B. cenocepacia* H111 (40). In the future, it would be interesting to test the ability of the compound to inhibit QS-regulated virulence in a genetic background where PAA-CoA synthesis is interrupted.

In the *paaK* knockout background the QS mutations had opposing effects. While a *cepI* deletion resulted in the expected attenuated virulence, a *cepR* deletion had wild-type levels of virulence. Surprisingly, the PAA pathway mutants with a *cepI* deletion had increased transcription of *cepR*. Therefore, it seems that extracellular PAA, observed in both PAA pathway mutants, can restore the transcription of *cepR* to wild-type levels. While increased transcription of *cepR* by PAA may suggest that this is the reason why the *paaK* mutants are more pathogenic than the wild type, it does not explain why PAA does not produce the same effect in the *paaABCDE* mutant, nor does it explain why the *cepR* mutation in a *paaK* background reverts to wild-type levels of virulence. A possible reason for these striking, opposite phenotypes is that in the *paaK* mutants a regulatory component is activated in the absence of CepR. We speculate that this activation is sensitive to the levels of PAA-CoA. However, a limitation of our work is that we were unable to detect statistically significant differences between the levels of PAA-CoA in the wild type and the PaaK mutants as the amounts of PAA-CoA were very close to the limit of detection of our method.

Finally, the results presented here highlight how changes in a catabolic pathway can modulate virulence in bacteria. Variations in the concentration of PAA-CoA led to CepR-dependent attenuated virulence, despite the presence of CepR. Conversely, the same virulence factors could increase, despite the absence of CepR. We propose that increased virulence due to PAA metabolites may be relevant under environmental conditions where quorum sensing signals do not accumulate but a virulent response is necessary.

MATERIALS AND METHODS

Strains, medium preparation, and growth conditions. Bacterial strains, listed in Table 2, were grown at 37°C with agitation at 230 rpm in lysogeny broth (LB) Lennox medium (without glucose) (43), unless specified otherwise. All cultures were started from isolated colonies grown 48 h on LB agar at 37°C, unless specified otherwise. Plasmids used are listed in Table 3. For *E. coli* strains the following antibiotics and concentrations were used: ampicillin (100 μg/ml; 200 μg/ml for W14 strain), chloramphenicol (30 μg/ml), kanamycin (30 μg/ml; 40 μg/ml for MM290 strain), trimethoprim (50 μg/ml; 100 μg/ml for W14 strain), and tetracycline (20 μg/ml). For *B. cenocepacia* strains the following antibiotics and concentrations were used: trimethoprim (100 μg/ml), tetracycline (100 μg/ml), and gentamycin (50 μg/ml). Stock solutions of C_8-HSL (Sigma-Aldrich) were suspended in dimethyl sulfoxide (DMSO) and stored at −20°C. For assays with exogenous addition of C_8-HSL, cultures were grown in LB medium supplemented

TABLE 2 Bacterial strains used in this study

Strain	Description	Reference(s) or source
Burkholderia cenocepacia strains		
K56-2 (LMG18863)	Wild-type strain, ET12 clone related to cystic fibrosis clinical isolate J2315	60
Δ*paaABCDE* strain	Deletion of *paaABCDE* operon in K56-2	18
Δ*paaK1* strain	Deletion of *paaK* gene on chromosome 1 (BCAL0404) in K56-2	This study
Δ*paaK2* strain	Deletion of *paaK* gene on chromosome 2 (BCAM1711) in K56-2	This study
Δ*paaK1* Δ*paaK2* strain	Deletion of *paaK* gene on chromosome 2 (BCAM1711) in K56-2 Δ*paaK1*	This study
Δ*paaK2* Δ*paaK1* strain	Deletion of *paaK* gene on chromosome 1 (BCAL0404) in K56-2 Δ*paaK2*	This study
Δ*cepI* strain	Deletion of BCAM1870 in K56-2	This study
Δ*cepR* strain	Deletion of BCAM1868 in K56-2	This study
Δ*paaABCDE* Δ*cepI* strain	Deletion of BCAM1870 in K56-2 Δ*paaABCDE*	This study
Δ*paaABCDE* Δ*cepR* strain	Deletion of BCAM1868 in K56-2 Δ*paaABCDE*	This study
Δ*paaK1* Δ*paaK2* Δ*cepI* strain	Deletion of BCAM1870 in K56-2 Δ*paaK1* Δ*paaK2*	This study
Δ*paaK1* Δ*paaK2* Δ*cepR* strain	Deletion of BCAM1868 in K56-2 Δ*paaK1* Δ*paaK2*	This study
Δ*paaK2* Δ*paaK1* Δ*cepI* strain	Deletion of BCAM1870 in K56-2 Δ*paaK2* Δ*paaK1*	This study
Δ*paaK2* Δ*paaK1* Δ*cepR* strain	Deletion of BCAM1868 in K56-2 Δ*paaK2* Δ*paaK1*	This study
Escherichia coli strains		
OP50	Uracil auxotroph	*Caenorhabditis* Genetic Center[a]
MM290		
SY327 λpir	*araD* Δ(*lac pro*) *argE*(Am) *recA56 rifR nalA* λpir	61
W14	*E. coli* W with deletion encompassing PAA pathway genes	30, 31

[a]University of Minnesota, Minneapolis, MN, USA.

with 50 mM 3-(*N*-morpholino)propanesulfonic acid (MOPS) to prevent pH-dependent lactonolysis (44). Stock solutions of L-arabinose (Alfa Aesar; Fisher Scientific) and L-rhamnose (Sigma-Aldrich) were prepared at a concentration of 20% (wt/vol) in deionized water and filter sterilized. Stock solutions of phenylalanine and PAA (Sigma-Aldrich) were prepared at 100 mM in deionized water, filter sterilized, and stored at room temperature. Stock solutions of PAA-CoA (Sigma-Aldrich) were prepared at 3.5 mM in DMSO and stored at −80°C.

Molecular biology techniques. Genetic manipulation of *B. cenocepacia* K56-2 was performed via triparental matings with *E. coli* MM290/pRK2013 as a helper strain. Plasmids generated were maintained in *E. coli* SY327 λpir or DH5α Z-competent cells depending on their origin of replication. PCRs were performed with an Eppendorf Mastercycler EP gradient S thermocycler with either HotStar HiFidelity *Taq* polymerase (Qiagen) or *Taq* DNA polymerase (Qiagen). Conditions were optimized for each primer set; primers used are listed in Table 4. Restriction enzymes and T4 DNA ligase (New England Biolabs) were used as recommended by the manufacturer. PCR products and digested DNA were purified by a

TABLE 3 Plasmids used in this study

Plasmid	Description[a]	Reference or source
pRK2013	ori_{colE1}, RK2 derivative, Kan^r, *mob*$^+$ *tra*$^+$	62
pGPI-SceI	ori_{R6K}, I-SceI recognition sequence, Tmp^r	45
pDAI-SceI	DHFR promoter controlling e-I-SceI, Tet^r	45
pBAD30	ori_{p15A} *araC* P_{BAD} Amp^r	63
pTL5	pBAD30 containing CepR (BCAM1868) with Shine-Dalgarno region	This study
pBBR*lux*	*luxCDABE*-based promoter plasmid	64
pTL7	pBBR*lux* containing *cepI* promoter region (upstream of BCAM1870)	This study
pTL12	pBBR*lux* containing *araC* and P_{BAD} promoter	This study
pTL13	pBBR*lux* containing *dhfr* promoter region	This study
pTL17	pGPI-SceI containing custom gene fragment for the deletion of *paaK1* (BCAL0404) in K56-2	This study
pTL18	pGPI-SceI containing custom gene fragment for the deletion of *paaK2* (BCAM1711) in K56-2	This study
pTnMod-STp	ori_{pSC101}, Tn*5* inverted repeats, Tn*5* transposase, Tmp^r	65
pTL9	BglII restriction digest of pTnMod-STp to remove Tn*5* transposase	This study
pTL21	ori_{pSC101} *rhaR rhaS* P_{rhaB}, Tmp^r	This study
pTL22	pTL21 expressing rhamnose-inducible *paaK* (ECW_m1532)	This study
pAAD	15.4-kb region contains *paa* cluster from *E. coli* W	31
pSCrhaB2	ori_{pBBR1} *rhaR rhaS* P_{rhaB} *mob*$^+$, Tmp^r	48
pKF2	pSCrhaB2 expressing rhamnose-inducible *paaK2* (BCAM1711)	This study
pCP300	*cepI*::*luxCDABE* transcriptional promoter fusion in pMS402	47
pPromcepR	*cepR*::*luxCDABE* transcriptional promoter fusion in pMS402	47
pMS402	*luxCDABE*-based promoter reporter plasmid, Kan^r Tp^r	47
pDelCepR	pGPI-SceI containing the upstream and downstream regions of *cepR* for markerless deletion in K56-2	47
pDelCepI	pGPI-SceI containing the upstream and downstream regions of *cepI* for markerless deletion in K56-2	47

[a]Amp^r, ampicillin resistance; Kan^r, kanamycin resistance; Tmp^r, trimethoprim resistance; Tet^r, tetracycline resistance.

TABLE 4 Primers used in this study

Primer no.	Sequence (5′–3′)[a]	Restriction site	Template and location[b]
900	TGCAACTCGTACAACCT		K56-2 upstream of BCAL0404
901	CCTGTGATTTAGGTTCGC		K56-2 downstream of BCAL0404
902	AAGGGCGTGAACTATCC		K56-2 upstream of BCAM1711
903	TAGAACGGCACACCTC		K56-2 downstream of BCAM1711
980	GTTGACATGACGAACGCCAC		K56-2 upstream of BCAL0404
981	GACATGCCGACCAAGGAAGA		K56-2 downstream of BCAL0404
982	CCGTTCGAGTTGATGGACCT		K56-2 upstream of BCAM1711
983	CGCATCGAAAAAGCGCTTGA		K56-2 downstream of BCAM1711
1055	GTGACTCAT**ATG**ACTCACCCGACGCATC	NdeI	K56-2 start of BCAM1711
1056	TTGACTTCTAGACTTCAATTCACCCATCGAACAG	XbaI	K56-2 downstream of BCAM1711
848	CCGCCAGGCAAATTCTGTTT		pSCrhaB2 downstream of the MCS
920	GCTTTCTGATAGTTGTTGTGG		pDAI-SceI
921	AGGTTGTTCGGGATGG		pDAI-SceI
154	ACAGGAACACTTAACGGCTGACATG		External to the MCS on pGPI-SceI
1080	GACAAGGGTTCGATCCAG		pDelCepR
1081	GATGGCCATCACGTTGCT		pDelCepR
1082	CATGACTTCACCCTTGC		pDelCepI
1083	CTTCGATGAACTGCGC		pDelCepI
1112	GTTGGTAGGCATCCTGC		K56-2 start of BCAM1870
1113	GTCGGTCAATGCGTGTC		K56-2 downstream of BCAM1870
703	ATTAGAGAATTCGGAGAAAGAATGGAACTGCGC	EcoRI	K56-2 start of BCAM1868
704	TCTAATTCTAGATCAGGGTGCTTCGATGAGC	XbaI	K56-2 end of BCAM1868
712	TCTAATACTAGTTGGCGCTCTTTATAAGC	SpeI	K56-2 BCAM1870 promoter region
713	TTGATCGGATCC**TCA**GAGTTCGTGTGGCAACC	BamHI	K56-2 BCAM1870 promoter region
768	AAGTATGAGCTCCAAGCCGTCAATTGTC	SacI	pBAD30 P_{BAD} region
769	TAAGATACTAGTAACAGTAGAGAGTTGCG	SpeI	pBAD30 P_{BAD} region
770	AAGTATGAGCTCGACATAAGCCTGTTCGG	SacI	pTnMod-STp P_{dhfr} region
771	TAAGATACTAGTTCAGTTGGCTTCATCGCTAC	SpeI	pTnMod-STp P_{dhfr} region
750	TACGCCGAAATCAACGACCA		qPCR primer for BCAM0918 (*rpoD*)
751	ACTTCGGCTTCCTCTTCGAC		qPCR primer for BCAM0918 (*rpoD*)
1033	AAGTTTCGAGCGTGACCAGTTC		qPCR primer for BCAM1870 (*cepI*)
1034	AACAGCGACTTCAGCAGATACG		qPCR primer for BCAM1870 (*cepI*)
1035	CGGATTCGAATACTGCTGTTACGG		qPCR primer for BCAM1868 (*cepR*)
1036	CTCGATGTAGTTCTGCGCCTG		qPCR primer for BCAM1868 (*cepR*)

[a]Restriction sites are underlined, and stop codons are in boldface.
[b]MCS, multiple-cloning site.

QIAquick Gel or PCR purification kit (Qiagen) and plasmids were isolated using a QIAprep Miniprep kit (Qiagen).

Construction of unmarked deletion mutants in *B. cenocepacia*. Unmarked deletion mutants were created using the system developed by Flannagan et al. (45). Flanking regions of the target gene were synthesized as a custom gene fragment with XbaI and SmaI restriction sites (Integrated DNA Technologies, Inc.) (see Table S1 in the supplemental material for sequences). The fragment with regions flanking BCAL0404 (*paaK1*) and pGPI-SceI were digested and ligated to create pTL17, and pTL18 was created by insertion of the fragment with regions flanking BCAM1711 (*paaK2*). Each plasmid was introduced into wild-type K56-2 by triparental mating and were integrated into the genome by homologous recombination. Colonies were picked onto LB medium supplemented with trimethoprim and onto *Burkholderia cepacia* selective agar (BCSA) (46). Conjugates with a dull phenotype on BCSA were selected. The integration of the suicide plasmids was confirmed with primers 900/901 for pTL17 and primers 902/903 for pTL18. Then, pDAI-SceI, expressing I-SceI endonuclease, was introduced into K56-2::pTL17 and K56-2::pTL18 by triparental mating. The double-stranded break caused by the I-SceI endonuclease triggered a recombination event that resulted in a reversion of the conjugate to a wild-type allele or a deletion of the fragment between the two flanking regions. Potential conjugates were tetracycline resistant and trimethoprim sensitive. The deletion event was confirmed by PCR using primer set 980/981 for *paaK1* and 982/983 for *paaK2*. Positive clones were cured of the pDAI-SceI plasmid by sequential subculturing in LB medium. Loss of the plasmid was confirmed by the loss of tetracycline resistance using the replica plate method and PCR with primer set 920/921 for the absence of pDAI-SceI.

Once cured, the mutants were tested for growth defects by washing overnight cultures twice in phosphate-buffered saline (PBS), diluting to an optical density at 600 nm (OD_{600}) of 0.04 in 200 μl of LB medium in a clear 96-well plate in triplicate. Plates were incubated at 37°C in a Biotek Synergy II plate reader with continuous shaking for 24 h, and the OD_{600} was measured every hour. Deletions of *cepI* and *cepR* were performed in the wild-type and PAA pathway mutant backgrounds using the pDelCepI and pDelCepR plasmids created by Aubert et al. (47). Integration of the plasmids was confirmed using primer set 1082/154 for *cepI* deletions and 1080/154 for *cepR*. pDAI-SceI was introduced, and potential conjugates were selected on appropriate antibiotics; the deletion event was confirmed by PCR with primer sets 1112/1113 and 1080/1081 for *cepI* and *cepR*, respectively. Positive clones were cured of the pDAI-SceI plasmid and screened for the loss of the plasmid as described above.

Plasmid construction. To create pKF2, *paaK2* (BCAM1711) was amplified from genomic *B. cenocepacia* K56-2 DNA using primers 1055/1056 and restricted with XbaI and NdeI before ligation into similarly digested pSCrhaB2 (48). The plasmid construct was verified using primers 1055/848. To create the *E. coli* reporter system, *cepR* (BCAM1868) was amplified using primers 703/704, and the amplicon and pBAD30 were restricted with EcoRI and XbaI and then ligated to form pTL5. To construct a plasmid expressing the *luxCDABE* operon, the *cepI* promoter region including the first 15 codons of *cepI* was amplified, and an in-frame stop codon was added using primers 712 and 713. Plasmid pBBRlux and the amplicon were digested with SpeI and BamHI, and ligation then resulted in pTL7. Plasmids pTL12 and pTL13 were created in the same way with primers 768/769 for the P_{BAD} promoter and regulatory *araC* and primers 770/771 for the *dhfr* promoter region of pTnMod-STp. To create a plasmid that expressed PaaK and was compatible with the reporter strain, we had to use the pSC101 *ori*. pTL9 was created by digesting pTnMod-STp with BglII to remove the Tn*5* transposase, and then the rhamnose-inducible promoter and its regulatory genes were added to create pTL21 using primers 724 and 947. Using primers 725 and 726, the *paaK* ligase from *E. coli* W was amplified from pAAD (30) and restriction cloned into pTL21 to create pTL22.

Growth of *B. cenocepacia* strains on various carbon sources. One milliliter of culture from a 5-ml overnight culture in LB with appropriate antibiotics was washed in PBS twice, and the OD_{600} was adjusted to 0.08 in 1 ml of M9 with 25 mM glucose or M9 with 5 mM PAA. A 100-μl aliquot was added to each well of a clear 96-well plate together with 100 μl of the appropriate medium for a starting OD_{600} of 0.04 in triplicate. Plates were incubated at 37°C with aeration at 230 rpm, and the OD_{600} was read after 48 h of incubation. OD_{600} values were converted to 1-cm path length by prior calibration with a GeneQuant III 4283, version 4283V1.6.

Quantification of intracellular and extracellular levels of PAA and PAA-CoA by IP-RP-UHPLC-MS/MS. *B. cenocepacia* cultures were diluted 1:100 into 10 ml of LB in a 50-ml Erlenmeyer flask and incubated at 37°C with agitation at 230 rpm for 6 h until late exponential phase. Using the differential method (24, 25), 1 ml of culture was immediately transferred into weighed tubes containing 5 ml of 60% (vol/vol) methanol in water held at −40°C in an acetonitrile–dry-ice bath, vortexed, and returned to −40°C. Two milliliters of culture was drawn into a syringe equipped with a 0.45-μm-pore-size filter, and 1 ml of filtrate was immediately transferred into 5 ml of 60% (vol/vol) methanol in water held at −40°C in an acetonitrile–dry-ice bath, vortexed, and returned to −40°C. Tubes were weighed, and 500 μl was transferred to a fresh tube and held at −40°C. Five milliliters of 75% (vol/vol) ethanol was boiled at 95°C for 4 min and then poured into the tube with 500 μl of sample, mixed, and placed at 95°C for 3 min. Extracted samples were then put back at −40°C and evaporated in a SpeedVac (Savant SC110 with refrigerated condensation trap RT100) until dry. Care was taken to ensure that the samples were not overdried. All measurements were carried out using ion-pair reversed-phase ultrahigh-performance liquid chromatography tandem mass spectrometry (IP-RP-UHPLC-MS/MS) as described previously (26), with slight modifications. Briefly, no splitter or makeup flow was used, and the chromatographic separation was performed on a narrower column (1 by 100 mm) with a lower eluant flow (0.075 ml/min).

For the *E. coli* W14 CepR reporter assay strains, cultures were diluted 1:100 in 5 ml of LB supplemented with 50 mM MOPS and appropriate antibiotics and grown at 30°C and 230 rpm to an OD_{600} of ~0.3. Cultures were provided 0.5 mM PAA and 0.01% rhamnose to induce the expression of *paaK* to convert PAA to PAA-CoA. Cultures were incubated again until an OD_{600} of 0.6 and diluted back to an OD_{600} of 0.3 before incubation for 1.5 h to simulate the conditions of the reporter assay. Samples were immediately prepared using the differential method described above.

Slow-killing assays in *Caenorhabditis elegans*. Worms were propagated and maintained on nematode growth medium (NGM) agar (2.5 g peptone/liter) seeded with a lawn of *E. coli* OP50 at 16°C. Slow-killing assays were performed as described previously (18). Briefly, 60-mm petri plates filled with 10 ml of a modified NGM agar (3.5 g peptone/liter) were seeded with 50 μl of a stationary-phase culture adjusted to an OD_{600} of 1.7. Plates were incubated overnight at 37°C to allow formation of a bacterial lawn. Twenty to 40 hypochlorite-synchronized *C. elegans* DH26 nematodes at larval stage L4 were inoculated onto each plate and subsequently incubated at 25°C for the duration of the assay. Worms were scored as live or dead for a period of 7 days.

Exoprotease assays. Cells from an overnight culture were washed with PBS twice and adjusted to an OD_{600} of 1.0. Three microliters of culture was spotted on 2% skim milk agar plates or 2% skim milk agar supplemented with 2 mM phenylalanine. Plates were incubated at 37°C for 48 h. Plates were prepared in duplicate, and three biological replicates were performed. Proteolytic activity was measured as a zone of clearing surrounding the colony. Images were taken at 48 h, and the area of the zone of clearance was analyzed using ImageJ software (49). A scale was applied to the images, and a threshold analysis was used to determine the zone of clearance. The area of this zone was then calculated (minus the area of the colony).

CepI enzymatic assay. Heterologous expression and purification of *cepI* were performed according to the conditions described previously (32). CepI enzyme activity was determined spectrophotometrically by measuring *holo*-ACP formation with dichlorophenylindophenol (DCPIP; $\varepsilon = 19{,}100\ M^{-1}\ cm^{-1}$) using a previously described assay (32, 50). Reaction mixtures contained 50 mM HEPES (pH 7.5), 0.005% Nonidet P-40, 0.13 mM DCPIP, 70 μM C_8-ACP, and 4 μM CepI. After 10 min of preincubation of the mixture, the reaction was initiated by addition of 40 μM *S*-adenosyl methionine. The compounds were assayed in triplicate at a concentration of 200 μM.

Luminescence assays with a CepR reporter strain. The reporter assay was performed based on the assay described by McInnis and Blackwell (51), with slight modifications. Briefly, overnight cultures were prepared from glycerol stocks in LB with appropriate antibiotics and incubated overnight at 30°C with

agitation at 230 rpm. The culture was diluted 1:100 into 5 ml of fresh LB medium supplemented with 50 mM MOPS and appropriate antibiotics. This subculture was incubated at 30°C with shaking at 230 rpm until it reached an OD_{600} of 0.6. One hundred microliters of culture was plated into wells with 100 μl of the appropriate medium containing C_8-HSL, PAA, and arabinose as needed, resulting in a starting OD_{600} of 0.3. For the reporter strain with pTL22 (rhamnose-inducible *paaK*), the culture was grown and subcultured as described above. This subculture was incubated at 30°C with shaking at 230 rpm until it reached an OD_{600} of ~0.3. At this time 0.5 mM PAA and 0.01% rhamnose were added to induce *paaK* expression, resulting in the conversion of PAA to PAA-CoA. The cultures were incubated at 30°C and 230 rpm until an OD_{600} of 0.6. One hundred microliters of culture was plated into wells with 100 μl of appropriate medium containing C_8-HSL, PAA, and arabinose and rhamnose as needed, resulting in a starting OD_{600} of 0.3. Arabinose and rhamnose were used at final concentrations of 0.2% (vol/vol) and 0.01% (vol/vol), respectively. C_8-HSL was used at a final concentration of 20 nM, which was the 50% effective concentration (EC_{50}) of C_8-HSL for the conditions of this assay as determined using a dose-response curve (see Fig. S1 in the supplemental material). PAA was tested at several concentrations (100 μM, 500 μM, 1 mM, and 5 mM), and PAA was added at 500 μM in the presence of 0.01% rhamnose to produce PAA-CoA. White 96-well microplates with clear bottoms were used, and the lids were treated with a Triton X-100–ethanol solution. Plates were incubated at 30°C with agitation in a Biotek Synergy 2 plate reader. The OD_{600} and relative luminescence were measured at 30-min intervals for 4 h. Inhibition was measured at the time point with peak signal intensity (2 h for PAA and 3 h for PAA-CoA).

Reverse transcription-quantitative PCR (RT-qPCR). Since quorum sensing is associated with cell density, the expression levels of quorum sensing genes are often measured during stationary phase (52–54). To study the expression of *cepI* and *cepR*, *B. cenocepacia* cells were harvested from stationary-phase cultures (OD_{600} of ~7). RNA was purified and DNase treated using a RiboPure bacteria kit (Ambion) with the DNase treatment extended to 2 h. RNA quality was confirmed by running the sample on a 2% agarose gel. cDNA was synthesized using an iScript reverse transcriptase kit (Bio-Rad) and quantified using iQ SYBR green Mastermix (Bio-Rad) performed on a CFX96 Touch real-time PCR detection system (Bio-Rad). Primer efficiency was calculated for each primer set, and efficiencies between 95% and 105% were deemed acceptable. Data were analyzed using the comparative threshold cycle (C_T) method (55, 56). Genes were normalized to the RNA polymerase sigma factor gene *rpoD* (BCAM0918; formerly known as *sigE*) as a reference gene (primers 750 and 751) (7, 57, 58).

LC-MS/MS quantification of AHLs. For AHL extraction, 5 ml of *B. cenocepacia* strain culture was harvested at the same time as the samples used for RT-qPCR (see the paragraph above). Samples were extracted and analyzed as described previously (59), and 5,6,7,8-tetradeutero-4-hydroxy-2-heptylquinoline (HHQ-d_4) was used as an internal standard at a concentration of 0.2 ppm.

SUPPLEMENTAL MATERIAL

Supplemental material for this article may be found at https://doi.org/10.1128/AEM.01594-19.

SUPPLEMENTAL FILE 1, PDF file, 4.3 MB.

ACKNOWLEDGEMENTS

This study was supported by a discovery grant from the Natural Sciences and Engineering Research Council of Canada awarded to S.T.C.

We acknowledge the preliminary work of Samuel J. Wolfram, Vincent Henega, and Stacey Line. We thank Miguel Valvano for generously sharing plasmids pDelCepR and pDelCepI. pBBRlux was a gift from Aleksandra Sikora.

T.J.L. and S.T.C. were responsible for the experimental design and writing the manuscript. T.J.L. and K.L.F. performed the experimental work. C.R. detected PAA and PAA-CoA using IP-RP-UHPLC-MS/MS. S.B. and L.R.C. performed the CepI enzyme activity assay. M.-C.G. and E.D. performed the LC-MS/MS and data analysis for AHL quantification. J.L.S. provided knowledge and equipment for the initial detection of PAA by HPLC and edited the manuscript.

REFERENCES

1. Bassler BL. 1999. How bacteria talk to each other: regulation of gene expression by quorum sensing. Curr Opin Microbiol 2:582–587. https://doi.org/10.1016/S1369-5274(99)00025-9.
2. Fuqua WC, Winans SC, Greenberg EP. 1994. Quorum sensing in bacteria: the LuxR-LuxI family of cell density-responsive transcriptional regulators. J Bacteriol 176:269–275. https://doi.org/10.1128/jb.176.2.269-275.1994.
3. Hanzelka BL, Greenberg EP. 1995. Evidence that the N-terminal region of the *Vibrio fischeri* LuxR protein constitutes an autoinducer-binding domain. J Bacteriol 177:815–817. https://doi.org/10.1128/jb.177.3.815-817.1995.
4. Winzer K, Williams P. 2001. Quorum sensing and the regulation of virulence gene expression in pathogenic bacteria. Int J Med Microbiol 291:131–143. https://doi.org/10.1078/1438-4221-00110.
5. Mahenthiralingam E, Urban TA, Goldberg JB. 2005. The multifarious, multireplicon *Burkholderia cepacia* complex. Nat Rev Microbiol 3:144–156. https://doi.org/10.1038/nrmicro1085.
6. Darling P, Chan M, Cox AD, Sokol PA. 1998. Siderophore production by cystic fibrosis isolates of *Burkholderia cepacia*. Infect Immun 66:874–877.
7. O'Grady EP, Viteri DF, Malott RJ, Sokol PA. 2009. Reciprocal regulation by the CepIR and CciIR quorum sensing systems in *Burkholderia cenocepacia*. BMC Genomics 10:441. https://doi.org/10.1186/1471-2164-10-441.
8. Malott RJ, Baldwin A, Mahenthiralingam E, Sokol PA. 2005. Characteriza-

tion of the *ccilR* quorum-sensing system in *Burkholderia cenocepacia*. Infect Immun 73:4982–4992. https://doi.org/10.1128/IAI.73.8.4982-4992.2005.
9. Lewenza S, Sokol PA. 2001. Regulation of ornibactin biosynthesis and *N*-acyl-L-homoserine lactone production by CepR in *Burkholderia cepacia*. J Bacteriol 183:2212–2218. https://doi.org/10.1128/JB.183.7.2212-2218.2001.
10. Lewenza S, Conway B, Greenberg EP, Sokol PA. 1999. Quorum sensing in *Burkholderia cepacia*: identification of the LuxRI homologs CepRI. J Bacteriol 181:748–756.
11. Malott RJ, O'Grady EP, Toller J, Inhülsen S, Eberl L, Sokol PA. 2009. A *Burkholderia cenocepacia* orphan LuxR homolog is involved in quorum-sensing regulation. J Bacteriol 191:2447–2460. https://doi.org/10.1128/JB.01746-08.
12. Brown SA, Palmer KL, Whiteley M. 2008. Revisiting the host as a growth medium. Nat Rev Microbiol 6:657–666. https://doi.org/10.1038/nrmicro1955.
13. Eisenreich W, Dandekar T, Heesemann J, Goebel W. 2010. Carbon metabolism of intracellular bacterial pathogens and possible links to virulence. Nat Rev Microbiol 8:401–412. https://doi.org/10.1038/nrmicro2351.
14. Fuchs TM, Eisenreich W, Heesemann J, Goebel W. 2012. Metabolic adaptation of human pathogenic and related nonpathogenic bacteria to extra- and intracellular habitats. FEMS Microbiol Rev 36:435–462. https://doi.org/10.1111/j.1574-6976.2011.00301.x.
15. de Lorenzo V. 2014. From the selfish gene to selfish metabolism: revisiting the central dogma. Bioessays 36:226–235. https://doi.org/10.1002/bies.201300153.
16. Bhuiyan MS, Ellett F, Murray GL, Kostoulias X, Cerqueira GM, Schulze KE, Mahamad Maifiah MH, Li J, Creek DJ, Lieschke GJ, Peleg AY. 2016. *Acinetobacter baumannii* phenylacetic acid metabolism influences infection outcome through a direct effect on neutrophil chemotaxis. Proc Natl Acad Sci U S A 113:9599–9604. https://doi.org/10.1073/pnas.1523116113.
17. Bartz FE, Glassbrook NJ, Danehower DA, Cubeta MA. 2012. Elucidating the role of the phenylacetic acid metabolic complex in the pathogenic activity of *Rhizoctonia solani* anastomosis group 3. Mycologia 104:793–803. https://doi.org/10.3852/11-084.
18. Pribytkova T, Lightly TJ, Kumar B, Bernier SP, Sorensen JL, Surette MG, Cardona ST. 2014. The attenuated virulence of a *Burkholderia cenocepacia paaABCDE* mutant is due to inhibition of quorum sensing by release of phenylacetic acid. Mol Microbiol 94:522–536. https://doi.org/10.1111/mmi.12771.
19. Teufel R, Mascaraque V, Ismail W, Voss M, Perera J, Eisenreich W, Haehnel W, Fuchs G. 2010. Bacterial phenylalanine and phenylacetate catabolic pathway revealed. Proc Natl Acad Sci U S A 107:14390–14395. https://doi.org/10.1073/pnas.1005399107.
20. Teufel R, Friedrich T, Fuchs G. 2012. An oxygenase that forms and deoxygenates toxic epoxide. Nature 483:359–362. https://doi.org/10.1038/nature10862.
21. Lightly TJ, Phung RR, Sorensen JL, Cardona ST. 2017. Synthetic cystic fibrosis sputum medium diminishes *Burkholderia cenocepacia* antifungal activity against *Aspergillus fumigatus* independently of phenylacetic acid production. Can J Microbiol 63:427–438. https://doi.org/10.1139/cjm-2016-0705.
22. Law RJ, Hamlin JNR, Sivro A, McCorrister SJ, Cardama GA, Cardona ST. 2008. A functional phenylacetic acid catabolic pathway is required for full pathogenicity of *Burkholderia cenocepacia* in the *Caenorhabditis elegans* host model. J Bacteriol 190:7209–7218. https://doi.org/10.1128/JB.00481-08.
23. Imolorhe IA, Silvia TC. 2011. 3-Hydroxyphenylacetic acid induces the *Burkholderia cenocepacia* phenylacetic acid degradation pathway. towards understanding the contribution of aromatic catabolism to pathogenesis. Front Cell Infect Microbiol 1:14. https://doi.org/10.3389/fcimb.2011.00014.
24. Taymaz-Nikerel H, de Mey M, Ras C, ten Pierick A, Seifar RM, van Dam JC, Heijnen JJ, van Gulik WM. 2009. Development and application of a differential method for reliable metabolome analysis in *Escherichia coli*. Anal Biochem 386:9–19. https://doi.org/10.1016/j.ab.2008.11.018.
25. Van Gulik WM, Canelas AB, Taymaz-Nikerel H, Douma RD, de Jonge LP, Heijnen JJ. 2012. Fast sampling of the cellular metabolome. Methods Mol Biol 881:279–306. https://doi.org/10.1007/978-1-61779-827-6_10.
26. Seifar RM, Ras C, Deshmukh AT, Bekers KM, Suarez-Mendez CA, da Cruz ALB, van Gulik WM, Heijnen JJ. 2013. Quantitative analysis of intracellular coenzymes in *Saccharomyces cerevisiae* using ion pair reversed phase ultra high performance liquid chromatography tandem mass spectrometry. J Chromatogr A 1311:115–120. https://doi.org/10.1016/j.chroma.2013.08.076.
27. Sokol PA, Sajjan U, Visser MB, Gingues S, Forstner J, Kooi C. 2003. The CepIR quorum-sensing system contributes to the virulence of *Burkholderia cenocepacia* respiratory infections. Microbiology 149:3649–3658. https://doi.org/10.1099/mic.0.26540-0.
28. Uehlinger S, Schwager S, Bernier SP, Riedel K, Nguyen DT, Sokol PA, Eberl L. 2009. Identification of specific and universal virulence factors in *Burkholderia cenocepacia* strains using multiple infection hosts. Infect Immun 9:4102–4110. https://doi.org/10.1128/IAI.00398-09.
29. Defoirdt T, Brackman G, Coenye T. 2013. Quorum sensing inhibitors: how strong is the evidence? Trends Microbiol 21:619–624. https://doi.org/10.1016/j.tim.2013.09.006.
30. Ferrandez A, Prieto MA, Garcia JL, Diaz E. 1997. Molecular characterization of PadA, a phenylacetaldehyde dehydrogenase from *Escherichia coli*. FEBS Lett 406:23–27. https://doi.org/10.1016/s0014-5793(97)00228-7.
31. Ferrandez A, Minambres B, Garcia B, Olivera ER, Luengo JM, Garcia JL, Diaz E. 1998. Catabolism of phenylacetic acid in *Escherichia coli*. Characterization of a new aerobic hybrid pathway. J Biol Chem 273:25974–25986. https://doi.org/10.1074/jbc.273.40.25974.
32. Scoffone VC, Chiarelli LR, Makarov V, Brackman G, Israyilova A, Azzalin A, Forneris F, Riabova O, Savina S, Coenye T, Riccardi G, Buroni S. 2016. Discovery of new diketopiperazines inhibiting *Burkholderia cenocepacia* quorum sensing in vitro and in vivo. Sci Rep 6:32487. https://doi.org/10.1038/srep32487.
33. Musthafa KS, Sivamaruthi BS, Pandian SK, Ravi AV. 2012. Quorum sensing inhibition in *Pseudomonas aeruginosa* PAO1 by antagonistic compound phenylacetic acid. Curr Microbiol 65:475–480. https://doi.org/10.1007/s00284-012-0181-9.
34. Wang J, Dong Y, Zhou T, Liu X, Deng Y, Wang C, Lee J, Zhang LH. 2013. *Pseudomonas aeruginosa* cytotoxicity is attenuated at high cell density and associated with the accumulation of phenylacetic acid. PLoS One 8:e60187. https://doi.org/10.1371/journal.pone.0060187.
35. Niu C, Clemmer KM, Bonomo RA, Rather PN. 2008. Isolation and characterization of an autoinducer synthase from *Acinetobacter baumannii*. J Bacteriol 190:3386–3392. https://doi.org/10.1128/JB.01929-07.
36. Latifi A, Winson MK, Foglino M, Bycroft BW, Stewart GS, Lazdunski A, Williams P. 1995. Multiple homologues of LuxR and LuxI control expression of virulence determinants and secondary metabolites through quorum sensing in *Pseudomonas aeruginosa* PAO1. Mol Microbiol 17:333–343. https://doi.org/10.1111/j.1365-2958.1995.mmi_17020333.x.
37. Yudistira H, McClarty L, Bloodworth RA, Hammond SA, Butcher H, Mark BL, Cardona ST. 2011. Phenylalanine induces *Burkholderia cenocepacia* phenylacetic acid catabolism through degradation to phenylacetyl-CoA in synthetic cystic fibrosis sputum medium. Microb Pathog 51:183–196. https://doi.org/10.1016/j.micpath.2011.04.002.
38. Sobotková L, Grafková J, Kyslík P. 2002. Effect of phenylacetic acid on the growth and production of penicillin G acylase of recombinant and host strains derived from *Escherichia coli* W. Enzyme Microb Technol 31:992–999. https://doi.org/10.1016/S0141-0229(02)00216-8.
39. Cui C, Yang C, Song S, Fu S, Sun X, Yang L, He F, Zhang L-H, Zhang Y, Deng Y. 2018. A novel two-component system modulates quorum sensing and pathogenicity in *Burkholderia cenocepacia*. Mol Microbiol 108:32–44. https://doi.org/10.1111/mmi.13915.
40. Cui C, Song S, Yang C, Sun X, Huang Y, Li K, Zhao S, Zhang Y, Deng Y. 2019. Disruption of quorum sensing and virulence in *Burkholderia cenocepacia* by a structural analogue of the cis-2-dodecenoic acid signal. Appl Environ Microbiol 85:e00105-19. https://doi.org/10.1128/AEM.00105-19.
41. Schmid N, Pessi G, Deng Y, Aguilar C, Carlier AL, Grunau A, Omasits U, Zhang L-H, Ahrens CH, Eberl L. 2012. The AHL- and BDSF-dependent quorum sensing systems control specific and overlapping sets of genes in *Burkholderia cenocepacia* H111. PLoS One 7:e49966. https://doi.org/10.1371/journal.pone.0049966.
42. Deng Y, Lim A, Wang J, Zhou T, Chen S, Lee J, Dong YH, Zhang LH. 2013. *cis*-2-Dodecenoic acid quorum sensing system modulates N-acyl homoserine lactone production through RpfR and cyclic di-GMP turnover in *Burkholderia cenocepacia*. BMC Microbiol 13:148. https://doi.org/10.1186/1471-2180-13-148.
43. Lennox ES. 1955. Transduction of linked genetic characters of the host by bacteriophage P1. Virology 1:190–206. https://doi.org/10.1016/0042-6822(55)90016-7.

44. Yates EA, Philipp B, Buckley C, Atkinson S, Chhabra SR, Sockett RE, Goldner M, Dessaux Y, Cámara M, Smith H, Williams P. 2002. *N*-Acylhomoserine lactones undergo lactonolysis in a pH-, temperature-, and acyl chain length-dependent manner during growth of *Yersinia pseudotuberculosis* and *Pseudomonas aeruginosa*. Infect Immun 70:5635–5646. https://doi.org/10.1128/iai.70.10.5635-5646.2002.
45. Flannagan RS, Linn T, Valvano MA. 2008. A system for the construction of targeted unmarked gene deletions in the genus *Burkholderia*. Environ Microbiol 10:1652–1660. https://doi.org/10.1111/j.1462-2920.2008.01576.x.
46. Henry DA, Campbell ME, LiPuma JJ, Speert DP. 1997. Identification of *Burkholderia cepacia* isolates from patients with cystic fibrosis and use of a simple new selective medium. J Clin Microbiol 35:614–619.
47. Aubert DF, O'Grady EP, Hamad MA, Sokol PA, Valvano MA. 2013. The *Burkholderia cenocepacia* sensor kinase hybrid AtsR is a global regulator modulating quorum-sensing signalling. Environ Microbiol 15:372–385. https://doi.org/10.1111/j.1462-2920.2012.02828.x.
48. Cardona ST, Valvano MA. 2005. An expression vector containing a rhamnose-inducible promoter provides tightly regulated gene expression in *Burkholderia cenocepacia*. Plasmid 54:219–228. https://doi.org/10.1016/j.plasmid.2005.03.004.
49. Schneider CA, Rasband WS, Eliceiri KW. 2012. NIH Image to ImageJ: 25 years of image analysis. Nat Methods 9:671–675. https://doi.org/10.1038/nmeth.2089.
50. Christensen QH, Grove TL, Booker SJ, Greenberg EP. 2013. A high-throughput screen for quorum-sensing inhibitors that target acyl-homoserine lactone synthases. Proc Natl Acad Sci U S A 110:13815–13820. https://doi.org/10.1073/pnas.1313098110.
51. McInnis CE, Blackwell HE. 2011. Thiolactone modulators of quorum sensing revealed through library design and screening. Bioorg Med Chem 19:4820–4828. https://doi.org/10.1016/j.bmc.2011.06.071.
52. O'Grady EP, Viteri DF, Sokol PA. 2012. A unique regulator contributes to quorum sensing and virulence in *Burkholderia cenocepacia*. PLoS One 7:e37611. https://doi.org/10.1371/journal.pone.0037611.
53. Chapalain A, Vial L, Laprade N, Dekimpe V, Perreault J, Déziel E. 2013. Identification of quorum sensing-controlled genes in *Burkholderia ambifaria*. MicrobiologyOpen 2:226–242. https://doi.org/10.1002/mbo3.67.
54. Uzelac G, Patel HK, Devescovi G, Licastro D, Venturi V. 2017. Quorum sensing and RsaM regulons of the rice pathogen Pseudomonas fuscovaginae. Microbiology 163:765–777. https://doi.org/10.1099/mic.0.000454.
55. Livak KJ, Schmittgen TD. 2001. Analysis of relative gene expression data using real-time quantitative PCR and the $2^{-\Delta\Delta CT}$ method. Methods 25:402–408. https://doi.org/10.1006/meth.2001.1262.
56. Schmittgen TD, Livak KJ. 2008. Analyzing real-time PCR data by the comparative C_T method. Nat Protoc 3:1101–1108. https://doi.org/10.1038/nprot.2008.73.
57. Peeters E, Sass A, Mahenthiralingam E, Nelis H, Coenye T. 2010. Transcriptional response of *Burkholderia cenocepacia* J2315 sessile cells to treatments with high doses of hydrogen peroxide and sodium hypochlorite. BMC Genomics 11:90. https://doi.org/10.1186/1471-2164-11-90.
58. Wong Y-C, Abd El Ghany M, Ghazzali RNM, Yap S-J, Hoh C-C, Pain A, Nathan S. 2018. Genetic determinants associated with *in vivo* survival of *Burkholderia cenocepacia* in the *Caenorhabditis elegans* model. Front Microbiol 9:1118. https://doi.org/10.3389/fmicb.2018.01118.
59. Chapalain A, Groleau M-C, Le Guillouzer S, Miomandre A, Vial L, Milot S, Déziel E. 2017. Interplay between 4-hydroxy-3-methyl-2-alkylquinoline and *N*-acyl-homoserine lactone signaling in a *Burkholderia cepacia* complex clinical strain. Front Microbiol 8:1021. https://doi.org/10.3389/fmicb.2017.01021.
60. Mahenthiralingam E, Coenye T, Chung JW, Speert DP, Govan JR, Taylor P, Vandamme P. 2000. Diagnostically and experimentally useful panel of strains from the *Burkholderia cepacia* complex. J Clin Microbiol 38:910–913.
61. Miller VL, Mekalanos JJ. 1988. A novel suicide vector and its use in construction of insertion mutations: osmoregulation of outer membrane proteins and virulence determinants in *Vibrio cholerae* requires *toxR*. J Bacteriol 170:2575–2583. https://doi.org/10.1128/jb.170.6.2575-2583.1988.
62. Figurski DH, Helinski DR. 1979. Replication of an origin-containing derivative of plasmid RK2 dependent on a plasmid function provided in trans. Proc Natl Acad Sci U S A 76:1648–1652. https://doi.org/10.1073/pnas.76.4.1648.
63. Guzman LM, Belin D, Carson MJ, Beckwith J. 1995. Tight regulation, modulation, and high-level expression by vectors containing the arabinose PBAD promoter. J Bacteriol 177:4121–4130. https://doi.org/10.1128/jb.177.14.4121-4130.1995.
64. Zielke RA, Simmons RS, Park BR, Nonogaki M, Emerson S, Sikora AE. 2014. The type II secretion pathway in *Vibrio cholerae* is characterized by growth phase-dependent expression of exoprotein genes and is positively regulated by σ^E. Infect Immun 82:2788–2801. https://doi.org/10.1128/IAI.01292-13.
65. Dennis JJ, Zylstra GJ. 1998. Plasposons: modular self-cloning minitransposon derivatives for rapid genetic analysis of gram-negative bacterial genomes. Appl Environ Microbiol 64:2710–2715.